

Tuning CPL by helical pitch modulation in helically-flexible small organic multichromophores

César Ray,^a Carolina Díaz-Norambuena,^b Mizuki Johnson,^c Florencio Moreno,^a Beatriz L. Maroto,^a Jorge Bañuelos,^b Gilles Muller,^c and Santiago de la Moya*^a

^a*Departamento de Química Orgánica, Facultad de Ciencias Químicas, Universidad Complutense de Madrid, Ciudad Universitaria s/n, 28040, Madrid, Spain. E-mail: santmoya@ucm.es*

^b*Departamento de Química Física, Universidad del País Vasco-EHU, Apartado 644, 48080, Bilbao, Spain.*

^c*Department of Chemistry, San José State University, San José, CA 95192-0101, USA.*

1. General methods, instrumentation and techniques	S2
2. Synthetic procedures and characterization data	S4
3. Photophysical and chiroptical properties	S5
4. ¹H and ¹³C NMR spectra	S10
5. References	S12

1. General methods, instrumentation and techniques

All reagents were used without purification. All solvents were of HPLC grade and were dried according to standard methods. Starting chemical substrates and reagents were used as commercially provided unless otherwise indicated. Thin-layer chromatography (TLC) was performed on silica gel and the chromatograms were visualized using UV light ($\lambda = 254$ or 365 nm). Flash column chromatography was performed using silica gel (230-400 mesh). ^1H , ^{13}C , ^{11}B and ^{19}F NMR spectra were recorded in CDCl_3 solution at 20°C , unless otherwise indicated. NMR chemical shifts are expressed in parts per million (δ scale). ^1H and ^{13}C NMR spectra are referenced to residual protons of CDCl_3 as internal standard ($\delta = 7.260$ and 77.16 ppm, respectively) and ^{11}B and ^{19}F NMR spectra are referenced to 15% $\text{BF}_3 \cdot \text{Et}_2\text{O}$ in CDCl_3 as external standard ($\delta = 0.00$ ppm) and $\text{C}_6\text{H}_5\text{CF}_3$ as external standard ($\delta = -63.0$ ppm), respectively. The type of carbon (C, CH, CH_2 or CH_3) was assigned by DEPT-135 NMR experiments. Additionally, complex spin-system signals were simulated by using MestReNova program version 10.0.1-14719. FTIR spectra were obtained from neat samples using the attenuated total reflection (ATR) technique. High-resolution mass spectrometry (HRMS) was performed using electrospray ionization (ESI) and hybrid quadrupole time-of-flight mass analyser (QTOF; positive-ion mode) for the detection. Optical rotations in chloroform solution (dye concentration, c , expressed in g/100 mL, *ca.* $0.1 \cdot 10^{-3}$, unless otherwise indicated) were recorded at 293 K on an Anton Paar MCP 100 polarimeter. Photophysical signatures were recorded using diluted dye solutions (*ca.* $2 \cdot 10^{-6}$ M) prepared from a concentrated stock solution in acetone (*ca.* 10^{-3} M), after vacuum evaporation of the solvent from a certain amount of sample, and ulterior dilution with the desired solvent of spectroscopic grade. UV-vis absorption and emission (fluorescence and excitation) spectra were recorded on a Varian (model CARY 4E) spectrophotometer and an Edinburgh Instrument spectrofluorometer (model FLSP 920), respectively. Fluorescence quantum yields (ϕ) were determined from corrected spectra (detector sensibility to the wavelength) by the optically dilute relative method and by the use of the following equation (Eq. 1), where A_{exc} is the absorbance at the excitation wavelength, $\int I d\lambda$ is the numerically integrated intensity from the luminescence spectra, and n is the index of refraction of the solution. The subscripts R and S denote reference and sample, respectively. PM567 in ethanol ($\phi = 0.84$)¹ was used as reference.

$$\frac{\phi_S}{\phi_R} = \frac{\int I_S d\lambda \frac{A_{R,\text{exc}}}{A_{R,S,\text{exc}}} \left(\frac{n_R}{n_S}\right)^2}{\int I_R d\lambda \frac{A_{R,\text{exc}}}{A_{R,S,\text{exc}}} \left(\frac{n_R}{n_S}\right)^2} \quad \text{Eq. 1}$$

The aforementioned spectrofluorimeter is also equipped with a wavelength-tunable pulsed Fianium laser. Thus, the Time Correlated Single-Photon Counting (TCSPC) technique was used to record the fluorescence decay curves. Fluorescence emission was monitored at the maximum emission wavelength after excitation by the said Fianium at the maximum absorption wavelength. The fluorescence lifetime (τ) was obtained from the slope of the exponential fit of the decay curve, after the deconvolution of the instrumental response

signal (recorded by means of a Ludox scattering suspension) by means of an iterative method. The goodness of the exponential fit was controlled by statistical parameters (chi-square and the analysis of the residuals). Ground state geometries were optimized at the density functional theory (DFT) level using the B3LYP hybrid functional and the double valence basis set with a polarization function (6-31g*). The geometries were considered as energy minimum when the corresponding frequency analysis did not afford any negative value. The solvent effect was also simulated during the calculations by the Self Consistent Reaction Field (SCRF) using the Polarizable Continuum Model (PCM). Chloroform was chosen as the solvent for the simulations, for a better comparison with the experimental measurements. All the optimizations were conducted without any geometrical restriction, and carried out in Gaussian 16 using a computational cluster provided by the SGIker resources of the UPV/EHU.

ECD spectra were recorded on a Jasco (model J-715) spectropolarimeter using standard quartz cells of 1-cm optical-path length in chloroform solution, at a dye concentration of *ca.* $3.5 \cdot 10^{-6}$ M.

Circularly polarized luminescence (CPL) and total luminescence spectra were recorded at 295 K in degassed chloroform solution, unless otherwise indicated, at a dye concentration of *ca.* $1.5 \cdot 10^{-3}$ M, on an instrument described previously,² operating in a differential photon-counting mode. The light source for excitation was a continuous wave 1000 W xenon arc lamp from a Spex Fluorolog-2 spectrofluorimeter, equipped with excitation and emission monochromators with dispersion of 4 nm/mm (SPEX, 1681B). To prevent artefacts associated with the presence of linear polarization in the emission,³ a high quality linear polarizer was placed in the sample compartment, and aligned so that the excitation beam was linearly polarized in the direction of emission detection (z-axis). The key feature of this geometry is that it ensures that the molecules that have been excited and that are subsequently emitting are isotropically distributed in the plane (x,y) perpendicular to the direction of emission detection. The optical system detection consisted of a focusing lens, long pass filter, and 0.22 m monochromator. The emitted light was detected by a cooled EMI-9558B photomultiplier tube operating in photo-counting mode.

2. Synthetic procedures and characterization data

Synthesis of bis(haloBODIPY) 1. BODIPY **1** was prepared according to the procedure described previously by us.⁴

Synthesis of bis(haloBODIPY) 3. Under argon atmosphere, a solution of 3,5-dichloro-4,4-difluoro-8-(4-methylphenyl)BODIPY **5**⁵ (50 mg, 0.14 mmol), (1*S*,2*S*)-1,2-bis(2-chlorophenyl)ethane-1,2-diamine dihydrochloride (25 mg, 0.07 mmol) and *N,N'*-diisopropylethanamine (3.6 mg, 0.28 mmol) in CH₃CN (3 mL) was stirred under reflux for 3 h. Then, water (15 mL) and CH₂Cl₂ (15 mL) were added, the organic layer was separated and the aqueous layer was extracted with CH₂Cl₂ (3×15 mL). The combined organic phases were washed with brine (1×15mL) and dried over anhydrous Na₂SO₄. After filtration and solvent evaporation under reduced pressure, the obtained residue was purified using flash chromatography (silica gel, hexane/CH₂Cl₂ 1:1) to obtain **3** (25 mg, 38%) as an orange solid. *R*_F = 0.31 (hexane/CH₂Cl₂ 4:6). [α]_D²⁰ 9163 (*c* 0.077 CHCl₃). ¹H NMR (CDCl₃, 300 MHz) δ 7.66 (br s, 2H), 7.35-7.04 (m, 4H), 7.22-7.09 (m, 12H), 6.73 (br s, 2H), 6.36 (d, *J* = 3.9 Hz, 2H), 6.18 (d, *J* = 3.9 Hz, 2H), 6.07 (br s, 2H), 5.73 (m, 2H), 2.40 (s, 6H) ppm. ¹³C NMR (CDCl₃, 75 MHz) δ 161.0 (C), 139.5 (C), 135.9 (br s, CH), 134.6 (C), 133.6 (C), 133.1 (C), 133.0 (C), 132.1 (C), 130.9 (C), 130.8 (C), 130.3 (CH), 130.2 (CH), 129.6 (br s, CH) (CH), 129.0 (CH), 128.0 (CH), 121.3 (CH), 113.1 (CH), 111.0 (CH), 59.1 (CH), 21.5 (CH₃) ppm. ¹¹B NMR (CDCl₃, 160 MHz) δ 0.86 (t, *J* = 33.1 Hz) ppm. ¹⁹F NMR (CDCl₃, 282 MHz) δ -147.8 (br s) ppm. FTIR ν 3342, 1590, 1488, 1411, 1093 cm⁻¹. HRMS (ESI⁺) *m/z*: [M+H]⁺ Calcd. for C₄₆H₃₅B₂Cl₄F₄N₆ 911.1770; Found 911.1788.

Synthesis of bis(haloBODIPY) 4. Following a similar procedure to that used for BODIPY **2**, 3,3-dichloro-4,4-difluoro-8-(4-methylphenyl)BODIPY **5**⁵ (50 mg, 0.14 mmol) was reacted with (1*S*,2*S*)-1,2-bis(2,4,6-trimethylphenyl)ethane-1,2-diamine dihydrochloride, using triethylamine (2.8 mg, 0.28 mmol) as the base. The reaction crude was purified using flash chromatography (silica gel, hexane/AcOEt 99:1) to obtain **4** (37 mg, 54%) as an orange solid. *R*_F = 0.30 (hexano/AcOEt 7:3). [α]_D²⁰ 13714 (*c* 0.088 CHCl₃). ¹H NMR (CDCl₃, 300 MHz) δ 7.30 (d, *J* = 7.6 Hz, 4H), 7.22 (d, *J* = 7.8 Hz, 4H), 7.14 (br s, 2H), 6.87-6.78 (m, 4H), 6.59 (m, 2H), 6.37 (d, *J* = 3.9 Hz, 2H), 6.15 (d, *J* = 3.9 Hz, 2H), 5.97 (d, *J* = 5.0 Hz, 2H), 5.61 (m, 2H), 2.74 (m, 6H), 2.41 (m, 6H), 2.18 (m, 6H), 1.78 (m, 6H) ppm. ¹³C NMR (CDCl₃, 75 MHz) δ 160.3 (C), 139.5 (C), 138.3(C), 136.9 (C), 136.32 (C), 136.28 (CH), 133.7 (C), 133.3 (C), 132.2 (C), 132.0 (CH), 131.0 (C), 130.5 (CH), 129.9 (CH), 129.0 (CH), 121.4 (CH), 113.1 (CH), 110.0 (CH), 57.0 (CH), 22.0 (CH₃), 21.5 (CH₃), 20.9 (CH₃), 20.2 (CH₃) ppm. ¹¹B NMR (CDCl₃, 160 MHz) 0.86 (t, *J* = 34.0 Hz) ppm. ¹⁹F NMR (CDCl₃, 282 MHz) -148.0 (dq, *J*_{F-F} = 104.3, *J*_{B-F} = 33.1 Hz), -148.7 (dq, *J*_{F-F} = 104.3, *J*_{B-F} = 33.1 Hz). FTIR ν 3396, 1608, 1584, 1409, 1088 cm⁻¹. HRMS (ESI⁺) *m/z*: [M+Na]⁺ Calcd. for C₅₂H₄₈B₂Cl₂F₄N₆Na 947.3337; Found 947.3365.

3. Photophysical and chiroptical properties

Table S1. Photophysical properties of the bis(haloBODIPY)s **1**, **3** and **4** in solvents of different polarity ($2 \cdot 10^{-6}$ M).

	Solvent	λ_{ab}^a (nm)	$\epsilon \cdot 10^{-4}^b$ ($M^{-1}cm^{-1}$)	λ_{fl}^c (nm)	ϕ^d	τ^e (ns)
1^f	c-Hexane	529.0	12.4	544.0	0.170	1.15 (97%); 4.70 (3%)
	CHCl ₃	525.5	8.3	544.5	0.140	0.23 (32%); 1.15 (68%)
	Acetone	508.5 469.5	5.5 5.8	537.5	0.005	-
	MeOH	511.0 469.5	5.4 5.5	535.5	0.000	-
3	c-Hexane	525.0 483.0	5.7 5.4	540.5	0.280	1.00 (86%); 2.55 (14%)
	CHCl ₃	527.0 483.0	5.1 4.9	544.0	0.040	0.08 (37%); 0.41 (48%); 1.11 (15%)
	Acetone	509.0 468.5	4.3 4.8	536.0	0.004	-
	MeOH	513.0 469.0	4.1 4.7	535.0	0.004	-
4	c-Hexane	533.0 484.5	5.3 7.1	547.0	0.250	0.71 (70%); 2.98 (30%)
	CHCl ₃	527.0 481.5	4.3 6.1	546.5	0.020	0.05 (54%); 0.23 (38%); 1.34 (8%)
	Acetone	505.0 468.5	4.1 5.7	535.0	0.004	-
	MeOH	514.0 471.0	4.2 6.1	538.5	0.003	-

^aMaximum absorption wavelength. ^bMaximum molar absorption; ^cMaximum fluorescence wavelength. ^dFluorescence quantum yield. ^eFluorescence lifetime. ^fData collected from ref. 4. c-Hexane: cyclohexane.

Table S2. Chiroptical signatures of bis(haloBODIPY)s **1**, **3** and **4** in chloroform.

	$[\alpha]_{\text{D}}^{20\text{ }a}$	$g_{\text{abs}} \cdot 10^3\text{ }^b$	$g_{\text{lum}} \cdot 10^3\text{ }^c$	$g_{\text{lum}}/g_{\text{abs}}$
1	5744 (<i>c</i> 0.070) ^d	+1.6 (230 nm)	-1.0 (570 nm) ^e	0.63
3	9163 (<i>c</i> 0.077)	+5.5 (531 nm)	+1.4 (610 nm)	0.25
4	13714 (<i>c</i> 0.088)	+13.2 (532 nm)	+2.1 (605 nm)	0.16

^aSpecific optical rotation (concentration *c* in g/100 mL within parentheses).

^bMaximum absorbance dissymmetry ratio (wavelength within parentheses).

^cMaximum luminescence dissymmetry factor (wavelength within parentheses).

^dData collected from ref. 4. ^eData collected from ref. 7.

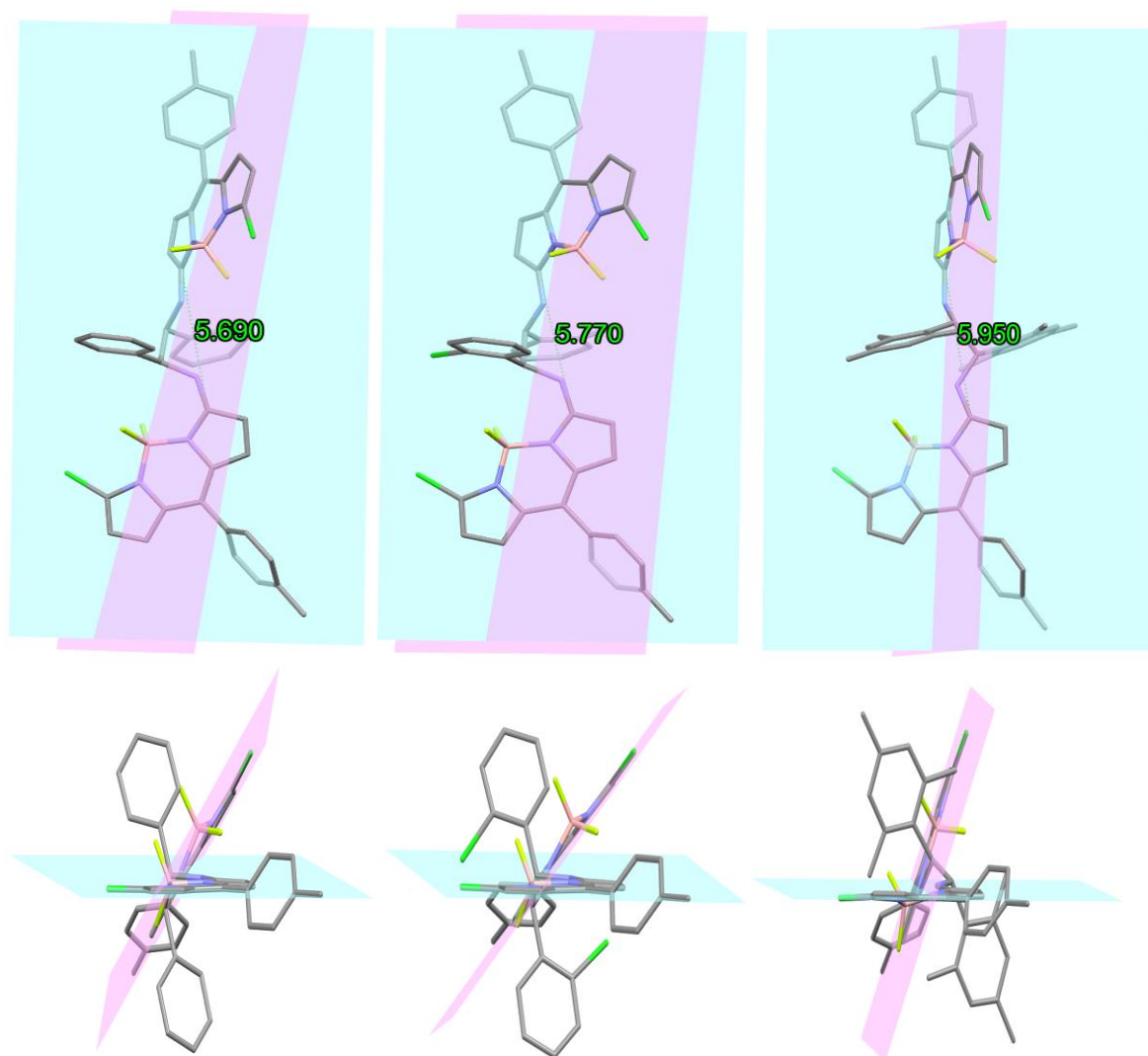


Figure S1. Ground-state optimized geometries in chloroform (PCM-B3LYP/6-31G*) of bis(haloBODIPY)s **1**, **3** and **4** (from left to right). d_{a-b} distance measuring the “pseudo” helical pitch (in nm; see main text), as well as the intersecting two planes generated by the transition dipole moments of each BODIPY subunit (in blue for the lower BODIPY; in pink for the upper BODIPY), in two different views (top and bottom).

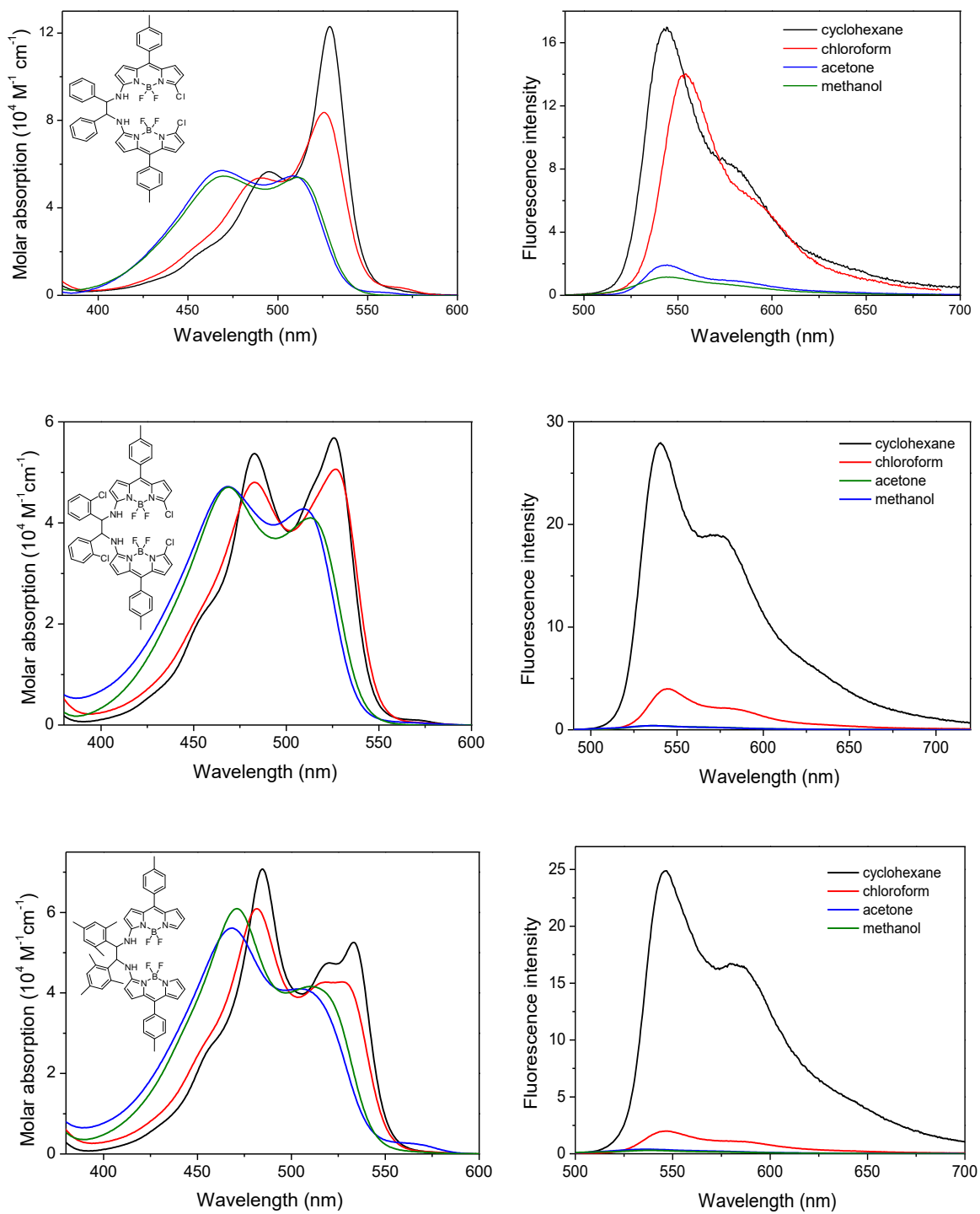


Figure S2. Visible absorption (left) and fluorescence (right) spectra of bis(haloBODIPY)s **1**, **3** and **4** (from top to bottom) in different solvents (2 μM).

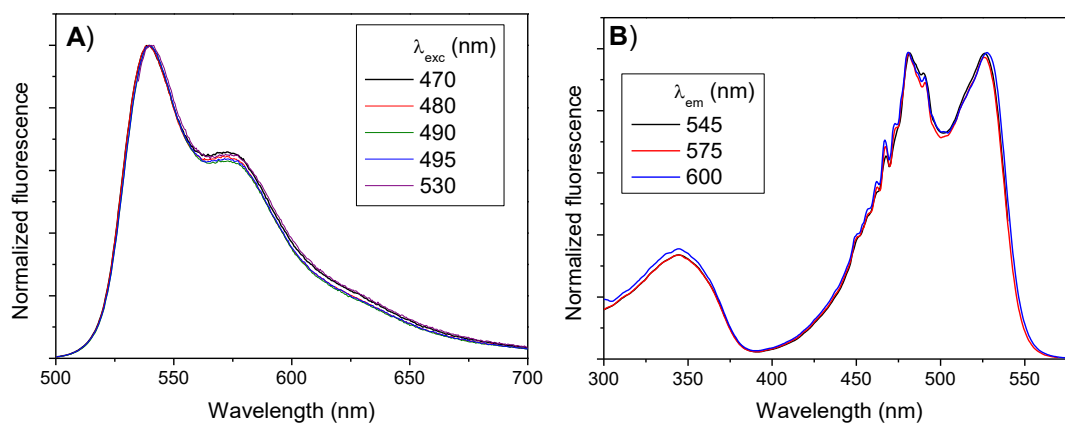


Figure S3. Fluorescence (A) and excitation (B) spectra at different excitation and emission wavelengths, respectively, for bis(haloBODIPY) **3** in cyclohexane.

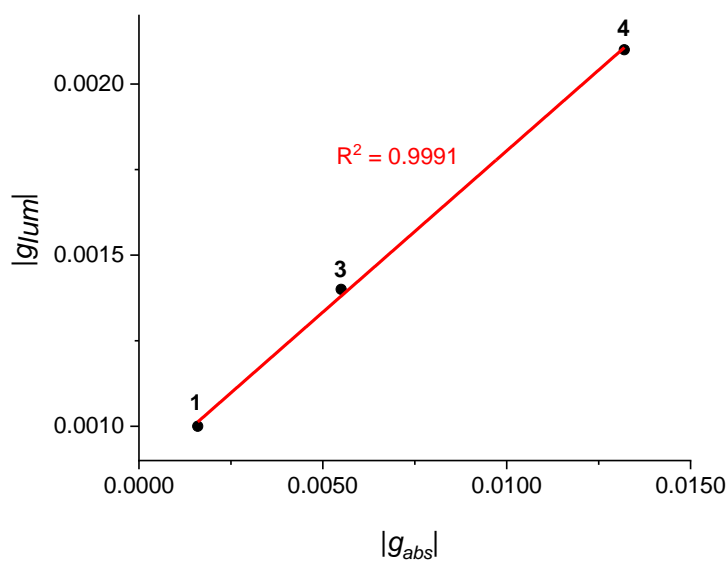
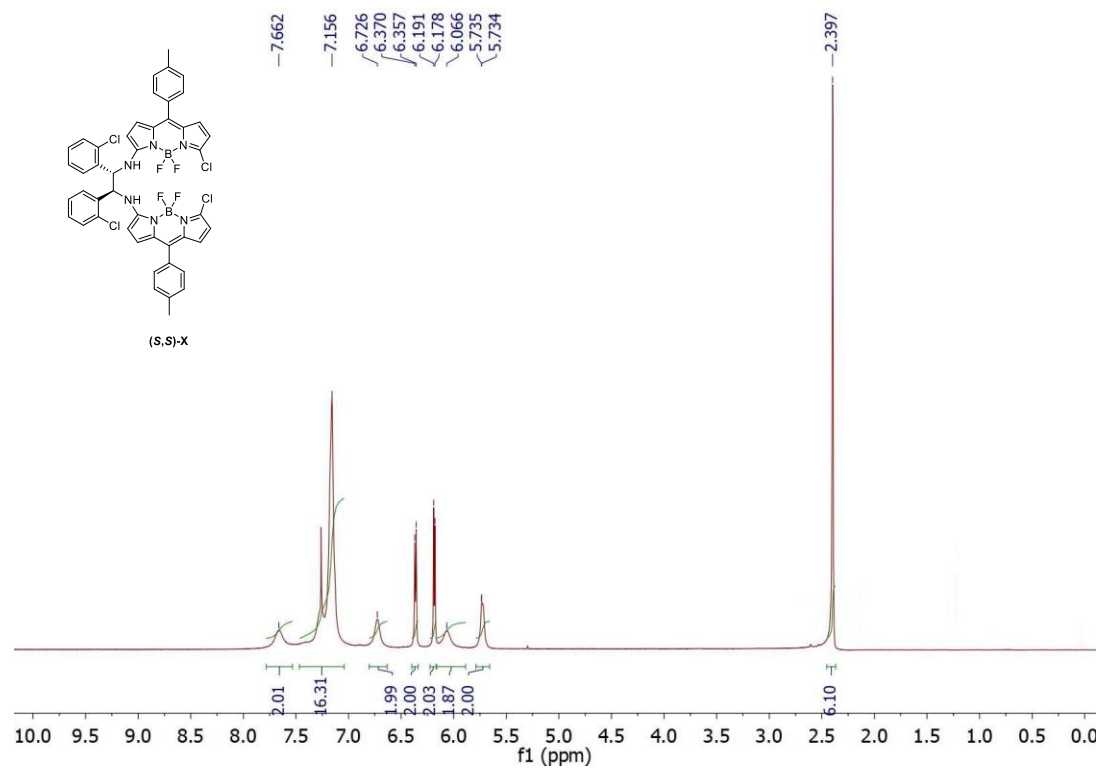


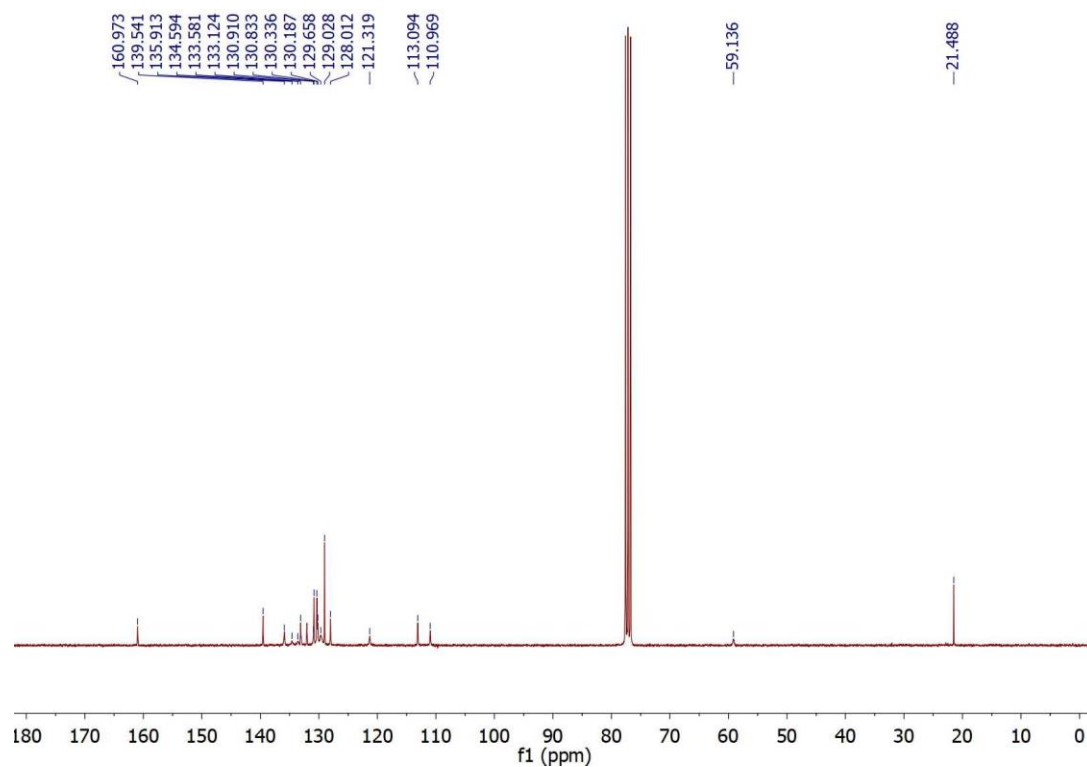
Figure S4. Linear correlation between maximum visible $|g_{lum}|$ in CHCl_3 vs. maximum visible $|g_{abs}|$ for bis(haloBODIPY)s **1**, **3** and **4** in CHCl_3 , and resulting linear regression coefficient (R^2).

4. ^1H and ^{13}C NMR spectra

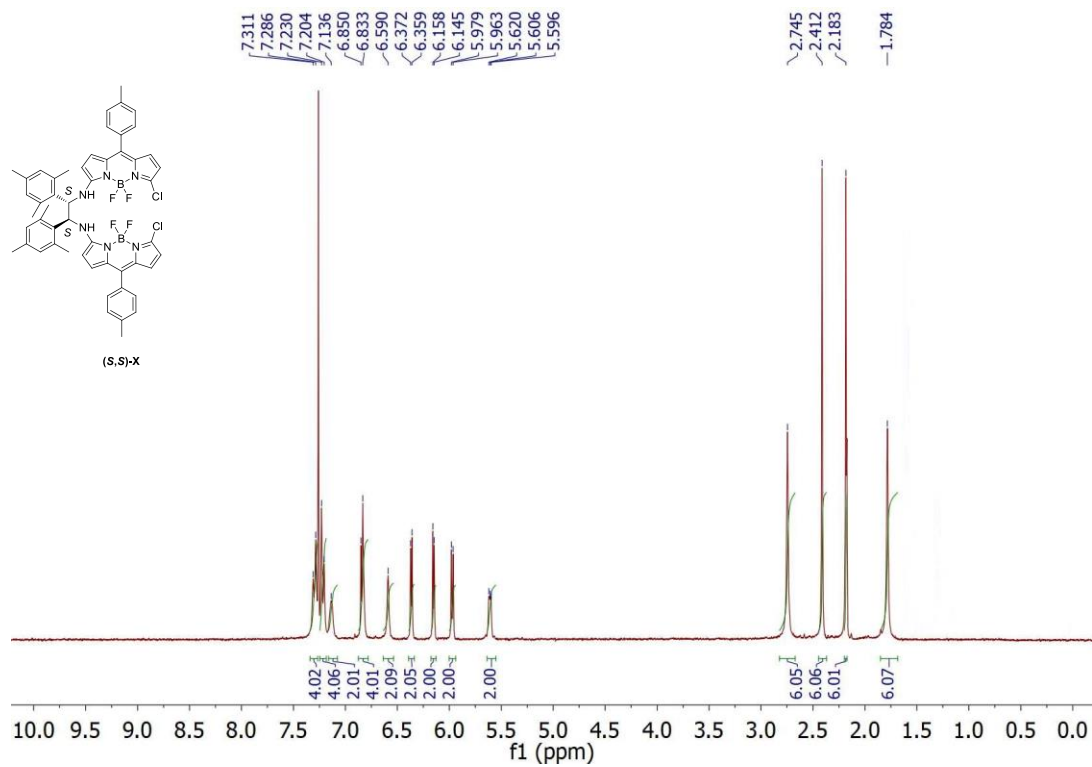
^1H NMR (300 MHz, CDCl_3) of 3.



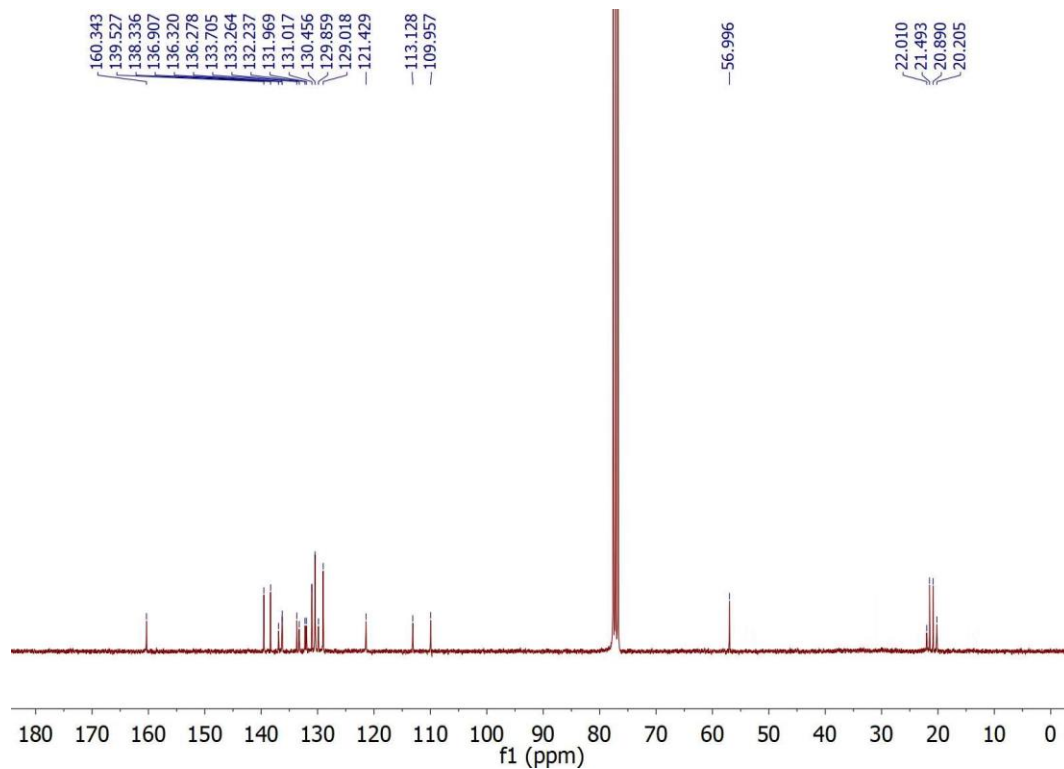
^{13}C NMR (75 MHz, CDCl_3) of 3.



¹H NMR (300 MHz, CDCl₃) of 4.



¹³C NMR (75 MHz, CDCl₃) of 4.



5. References

- [1] F. López Arbeloa, J. Bañuelos, V. Martínez, T. Arbeloa, I. López Arbeloa, *Int. Rev. Phys. Chem.* **2005**, *24*, 339-374.
- [2] E. Brunet, L. Jiménez, M. de Victoria-Rodríguez, V. Luu, G. Muller, O. Juanes, J. C. Rodríguez-Ubis, *Microporous Mesoporous Mater.* **2013**, *169*, 222-234, and references cited therein.
- [3] H. P. J. M. Dekkers, P. F. Moraal, J. M. Timper, J. P.; Riehl, *Appl. Spectrosc.* **1985**, *39*, 818-821.
- [4] E. M. Sánchez-Carnerero, F. Moreno, B. L. Maroto, A. R. Agarrabeitia, J. Bañuelos, T. Arbeloa, I. López-Arbeloa, M. J. Ortiz and S. de la Moya, *Chem. Commun.* **2013**, *49*, 11641-11643.
- [5] T. Rohand, M. Baruah, W. Qin, N. Boens and W. Dehaen, *Chem. Commun.* **2006**, 266-268.
- [6] L. Arrico, L. Di Bari and F. Zinna, *Chem. Eur. J.* **2020**, *27*, 2920-2934.
- [7] C. Ray, E. M. Sánchez-Carnerero, F. Moreno, B. L. Maroto, A. R. Agarrabeitia, M. J. Ortiz, I. López-Arbeloa, J. Bañuelos, K. D. Cohovi, J. L. Lunkley, G. Muller, S. de la Moya, *Chem. Eur. J.* **2016**, *22*, 8805-8808.